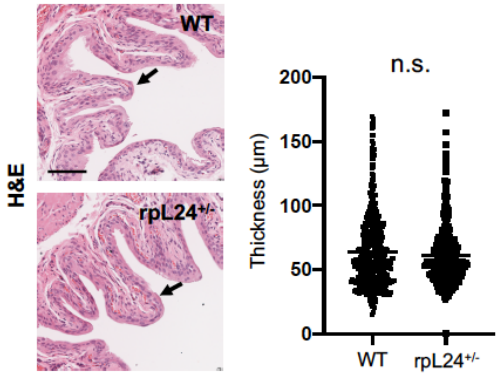

Figure S1. rpL24+/- bladders are histologically normal. Representative H&E staining of WT and rpL24+/- bladder urothelium (scale bar: 100 µm) with quantification (right panel, n = 3 mice/genotype, n.s. = not statistically significant).

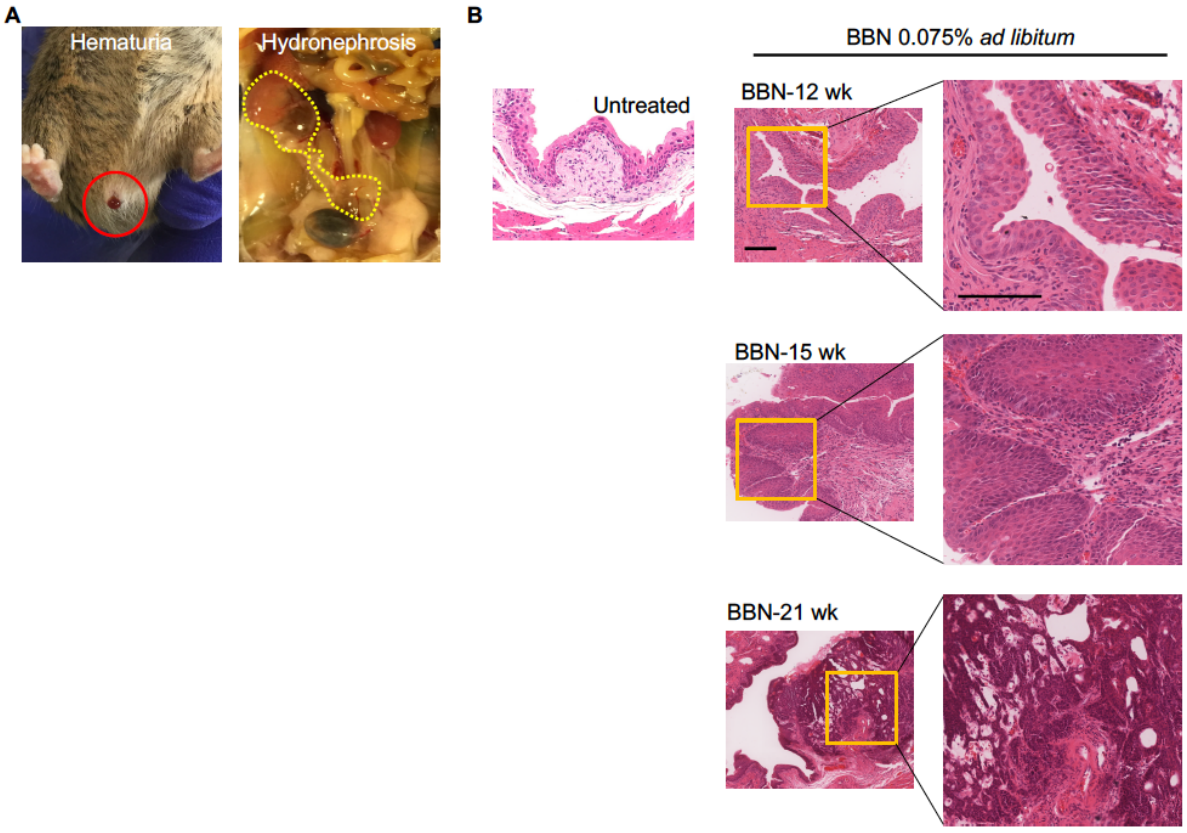

Figure S2. Gross and microscopic effects of BBN treatment in WT mice. (A) Representative gross images of mice treated with BBN of over 21 weeks that develop hematuria (demarcated by a red circle) and hydronephrosis (demarcated by a dotted yellow line). **(B)** H&E staining showing development of BBN-induced invasive bladder cancer in WT C57BL/6 mice (representative areas are shown at high magnification for clarity). All scale bars: 100 μm.

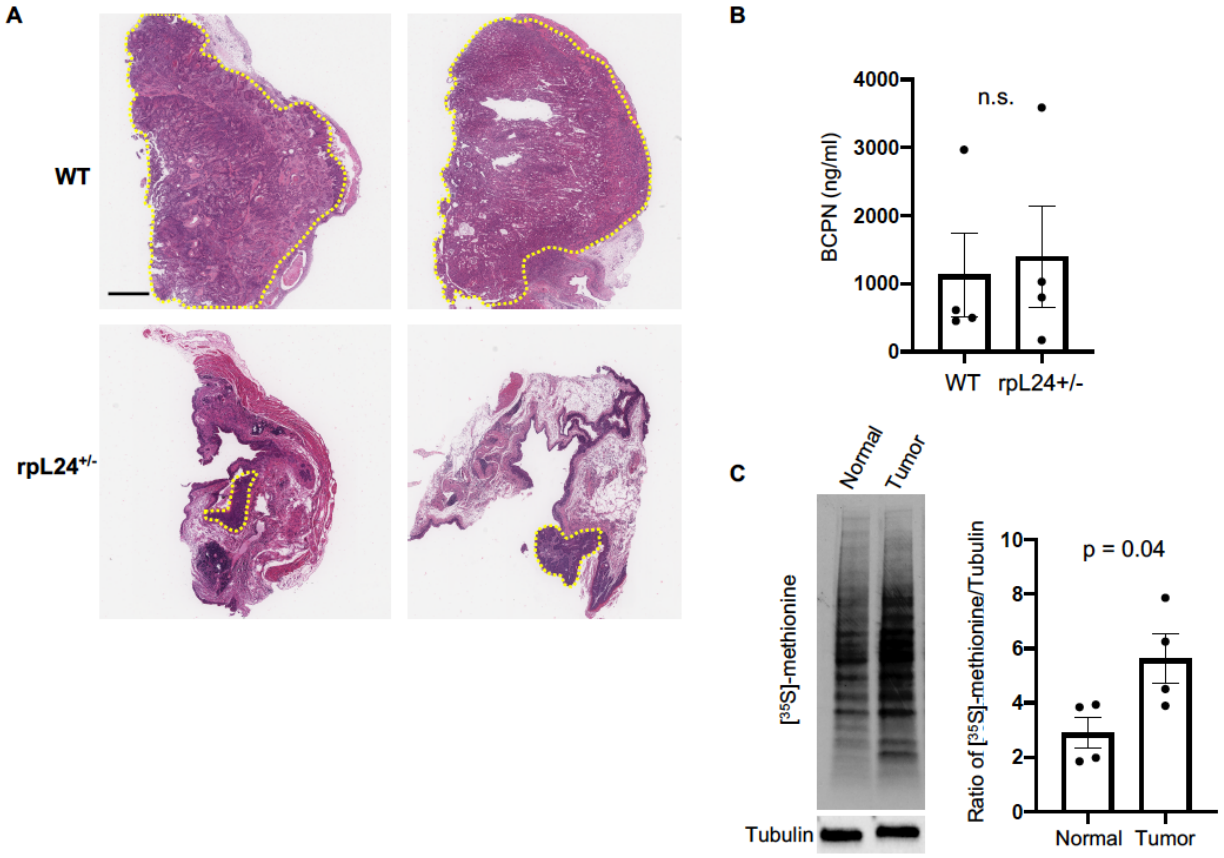

Figure S3. rpL24+/- mice exhibit smaller bladder tumors compared to WT mice but concentrate the carcinogen BCPN in urine at levels similar to WT mice and [^{35}S]-methionine incorporation in WT and BBN-induced tumor organoids. (A) Representative H&E staining showing tumor area of BBN-induced invasive bladder cancer in age-matched WT and rpL24$^{+/-}$ mice (all mice depicted were treated with BBN for 200 days, dotted yellow lines demarcate the bladder tumor, scale bar: 1 mm). **(B)** Bar graph representing mass spectrometry data of BCPN, the carcinogenic BBN metabolite, within the urine of WT and rpL24+/- mice (n = 4 mice/genotype). n.s. = not statistically significant. Data are presented as means +/- SEM**. (C)** [^{35}S]-methionine incorporation in WT and BBN-induced tumor organoids. *Left panel*: representative western blot. *Right panel*: quantification of n = 4 biological replicates (p = 0.04 , t-test). Data are presented as means +/- SEM**.**

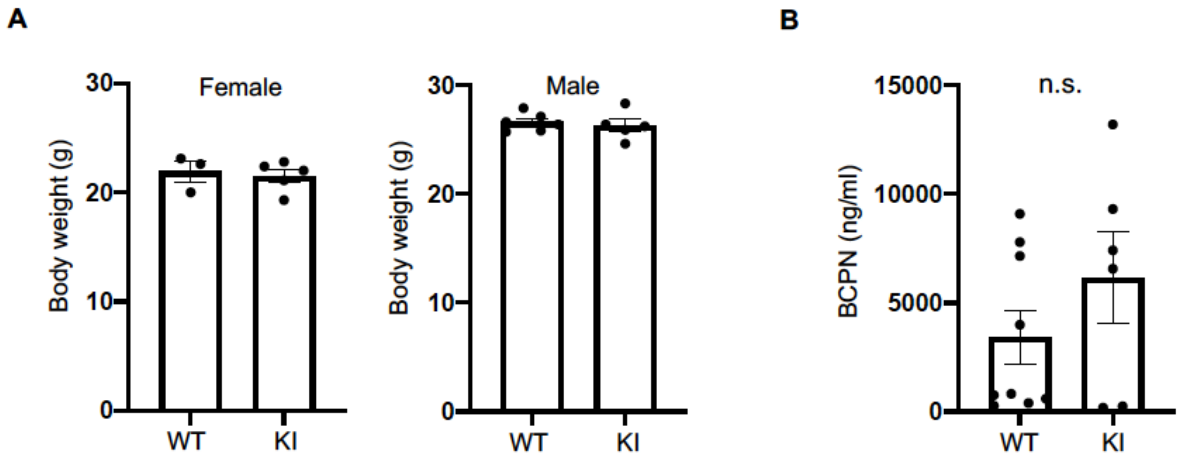

Figure S4. eIF4E$^{S209A/S209A}$ mouse weights and urine BCPN levels. (A) Body weight measurements of age-matched eIF4E$^{S209A/S209A}$ mice compared to WT mice. **(B)** WT and eIF4E$^{S209A/S209A}$ urine BCPN levels as determined by mass spectrometry (n = 6-9 mice/genotype). n.s. = not statistically significant. Data are presented as means +/- SEM.

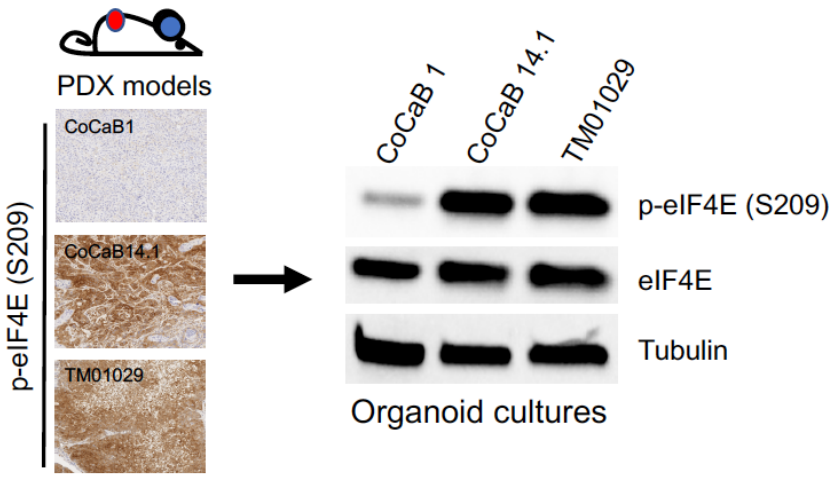

Figure S5. Comparison of IHC and western blot analysis of PDX models. PDX-derived primary tumor organoids reflect the phospho-eIF4E levels of the PDX models they are derived from. Comparison of eIF4E S209 phosphorylation levels between the CoCaB1, CoCaB14.1, and TM01029 PDX models and their respective organoids.

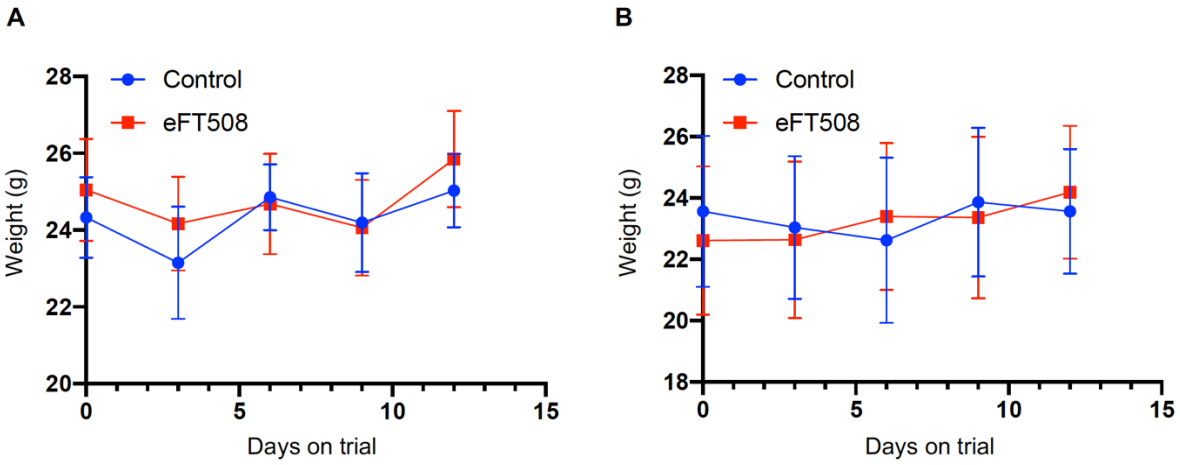

Figure S6. eFT508 treatment is well tolerated in PDX models. Weights of the TM01029 **(A)** and CoCaB1 **(B)** PDX models treated with eFT508 10mg/kg PO daily.

Figure 1C

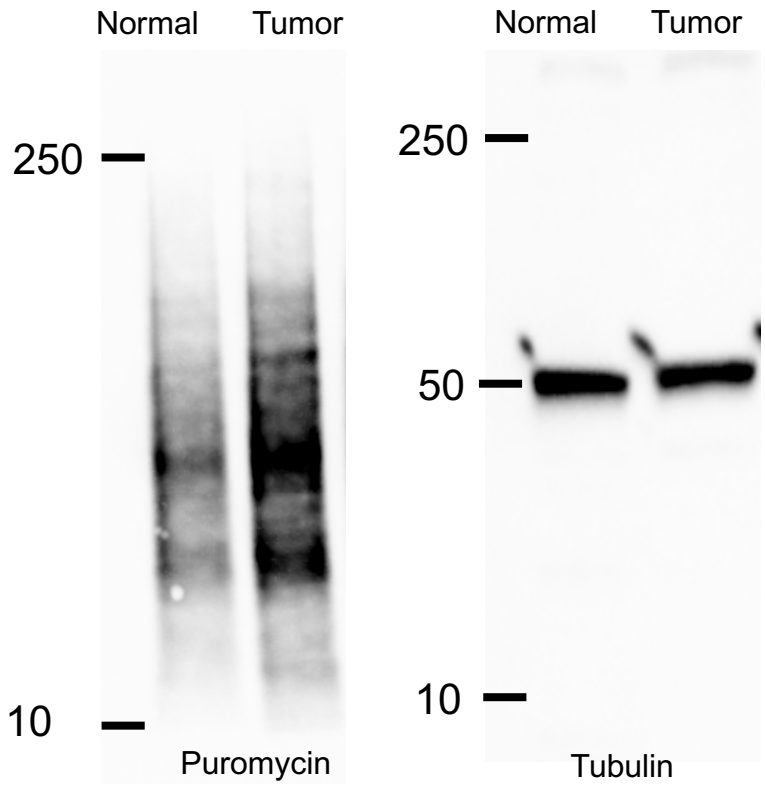
Normal
Tumor
250
10
Puromycin
Normal
Tumor
250
50
10
Tubulin

Figure 1D

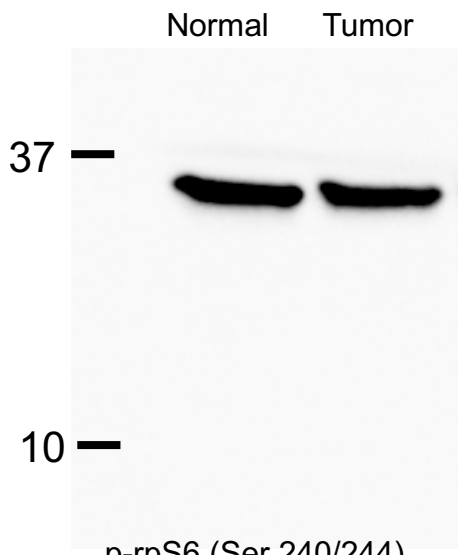

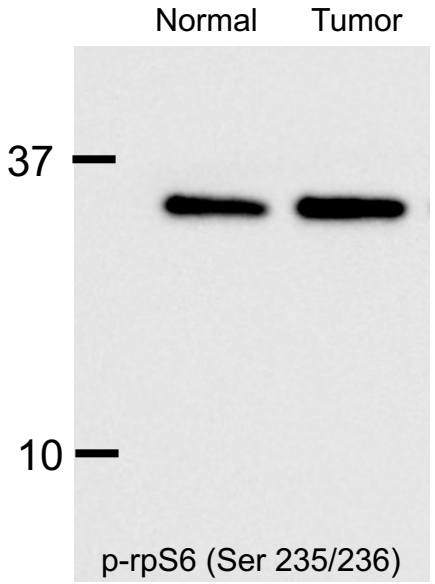

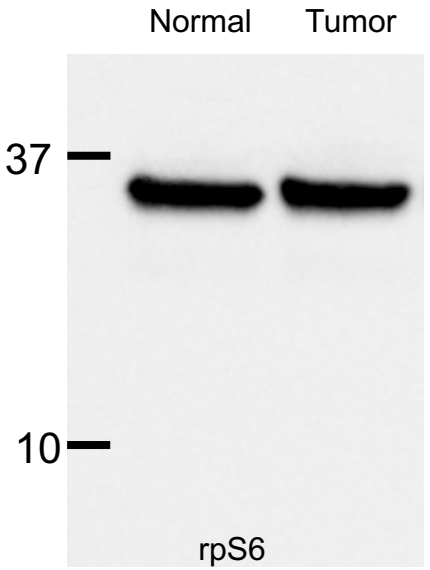

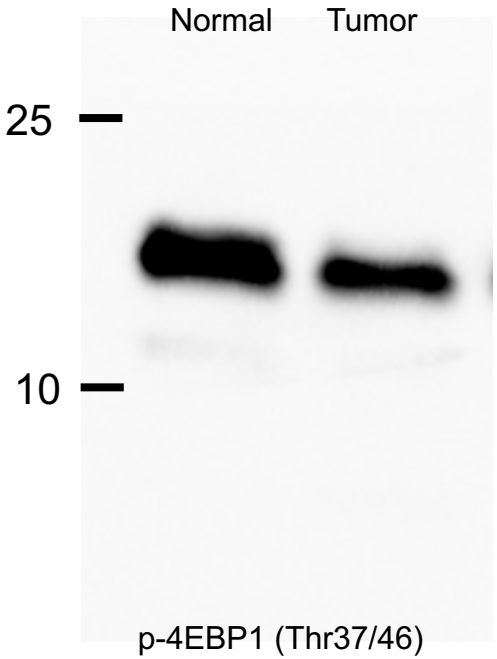

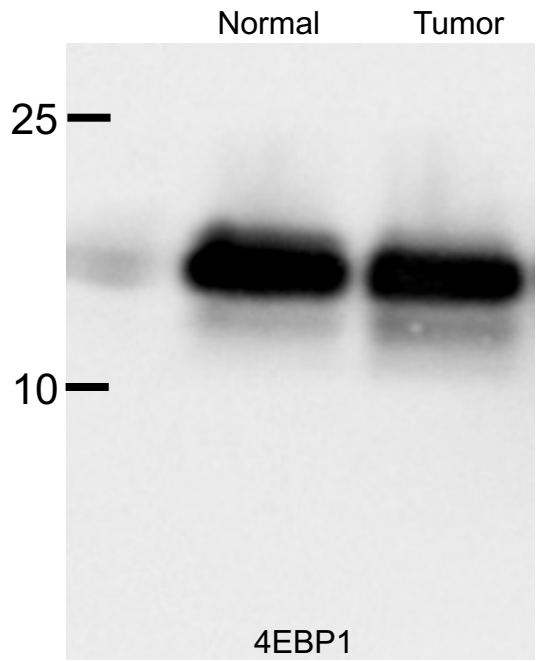

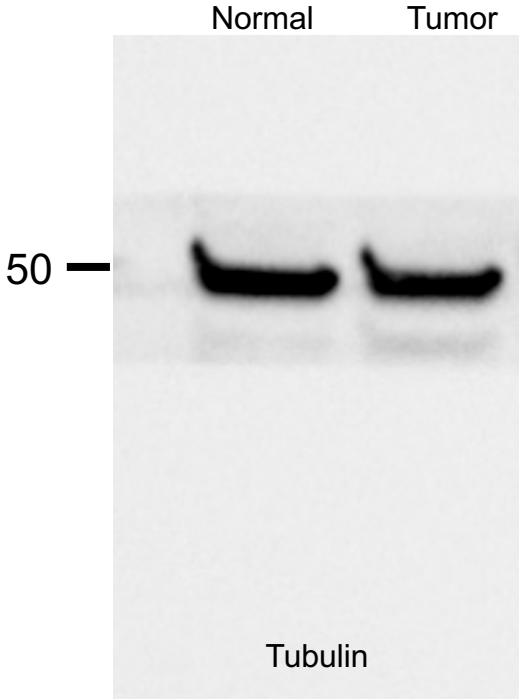

This tubulin blot was the loading control for all PI3K pathway and integrated stress response pathway blots.

Figure 1D

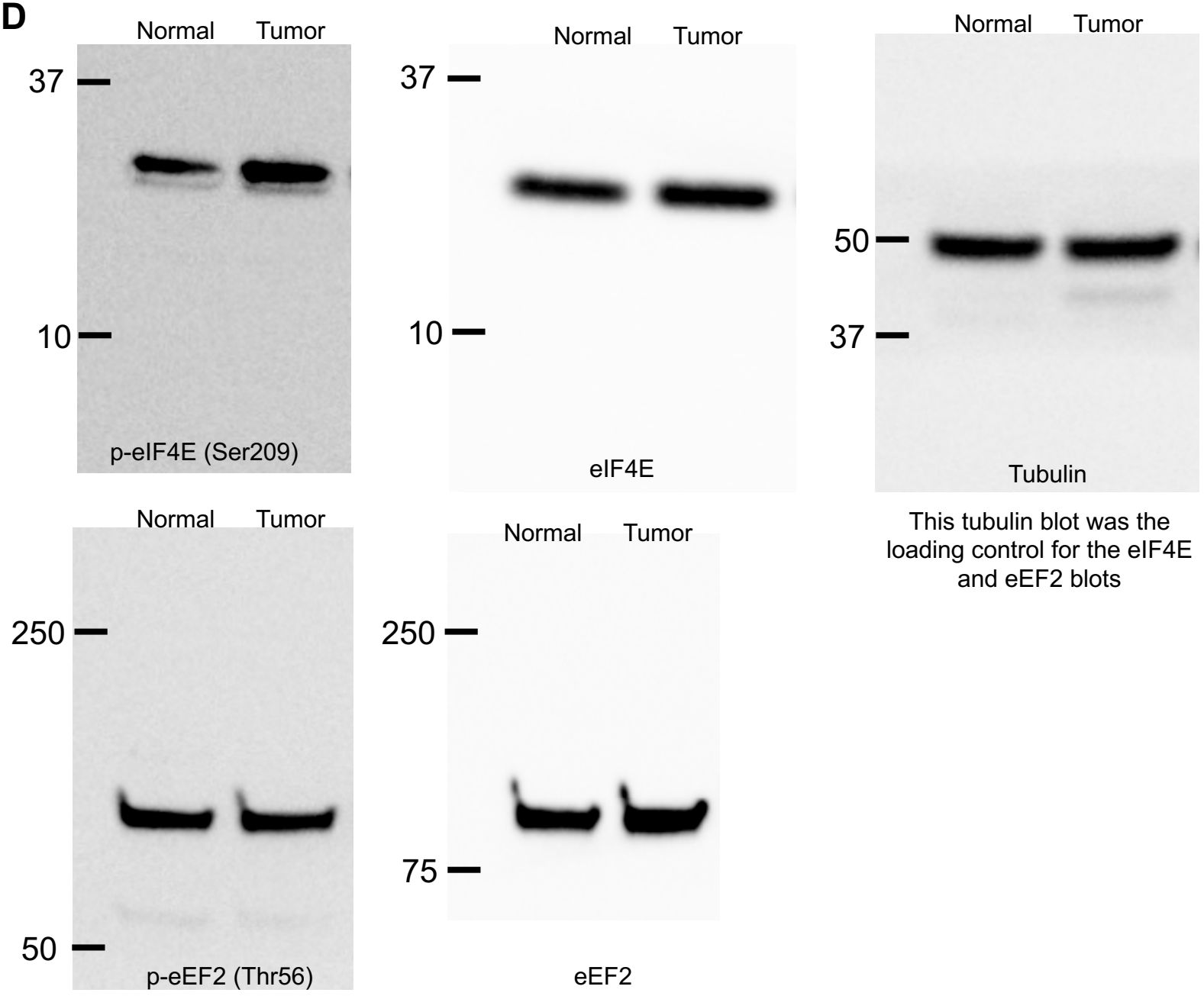

This tubulin blot was the loading control for the eIF4E and eEF2 blots

Figure 1D

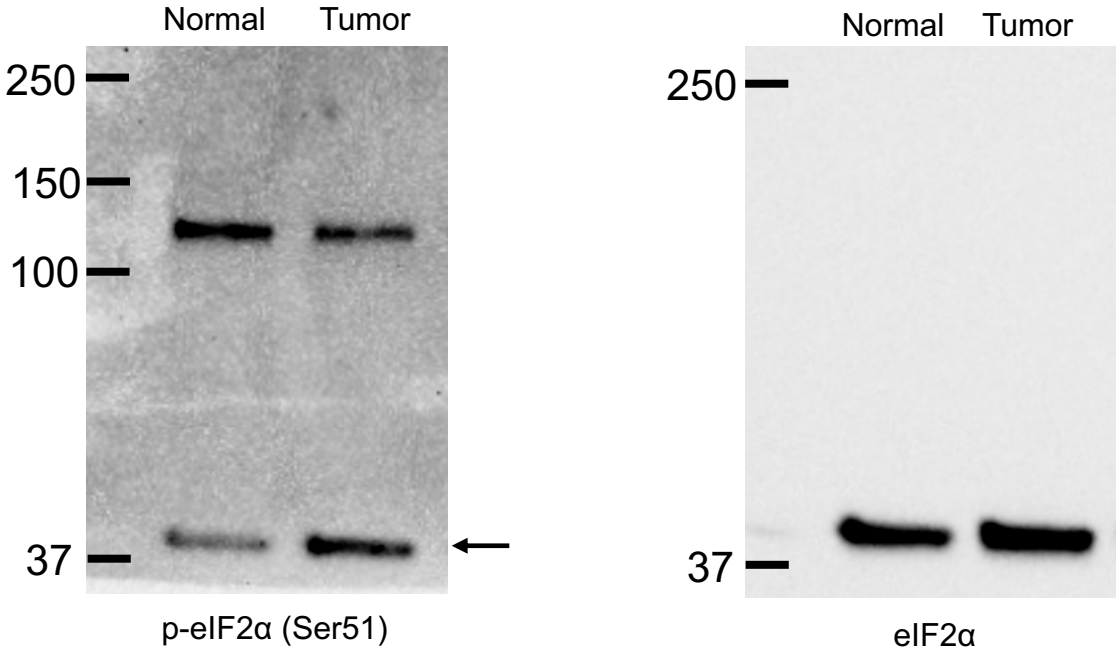
Normal
Tumor
250
150
100
37
p-eIF2α (Ser51)
Normal
Tumor
250
37
eIF2α

Figure 3C

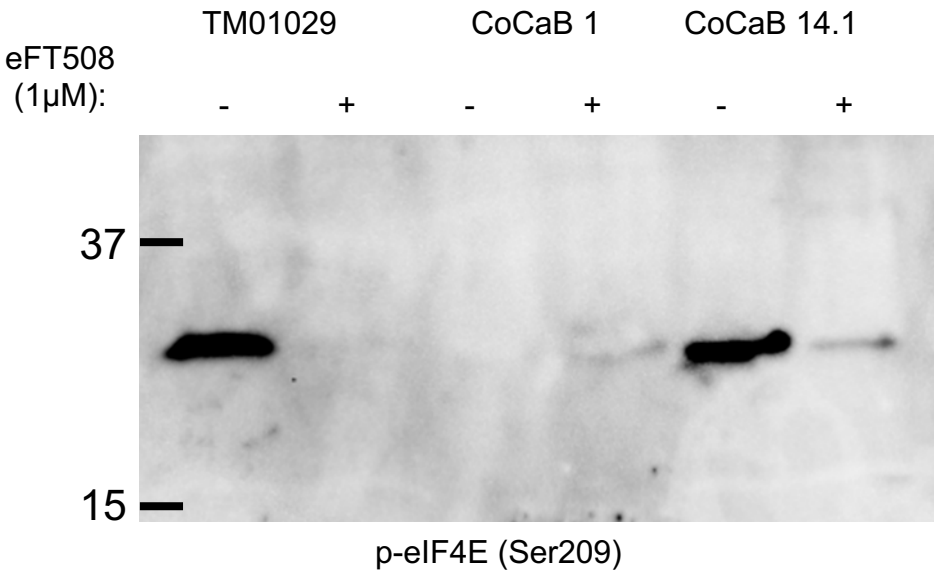
TM01029
CoCaB 1
CoCaB 14.1
eFT508
(1μM):
- + - + - +
37
15
p-eIF4E (Ser209)
TM01029
CoCaB 1
CoCaB 14.1
eFT508
(1μM):
- + - + - +
50
20
Tubulin

Supplemental Figure 3C

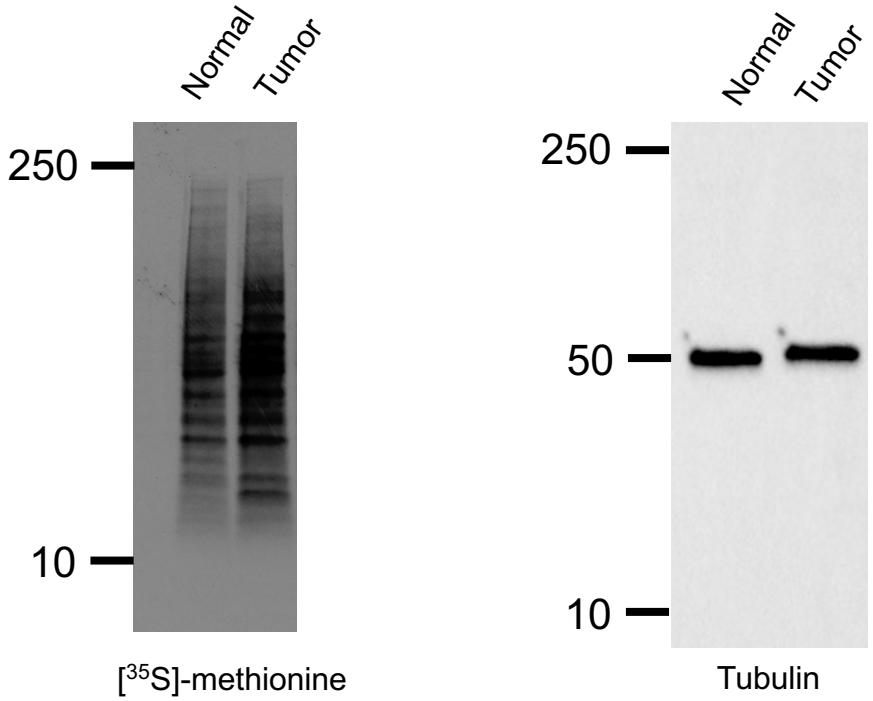

Supplemental Figure 5